Naval Research Laboratory

Washington, DC 20375-5000

NRL/MR/4790—92-6973

Tunable, Short Pulse Hard X-Rays from a Compact Laser Synchrotron Source

PHILLIP SPRANGLE, ANTONIO TING,
ERIC ESAREY, AND AMNON FISHER

Beam Physics Branch
Plasma Physics Division

July 16, 1992

REPORT DOCUMENTATION PAGE

Form Approved
OMB No. 0704-0188

1. AGENCY USE ONLY (Leave blank)	2. REPORT DATE	3. REPORT TYPE AND DATES COVERED
	July 16, 1992	Interim

4. TITLE AND SUBTITLE

Tunable, Short Pulse Hard X-rays from a Compact Laser Synchrotron Source

5. FUNDING NUMBERS

DOE Contract #
DOE-AI05-83ER40117

J.O. #47-0899-0-2

6. AUTHOR(S)

Phillip Sprangle, Antonio Ting, Eric Esarey, and Amnon Fisher

7. PERFORMING ORGANIZATION NAME(S) AND ADDRESS(ES)

Naval Research Laboratory
Washington, DC 20375-5000

8. PERFORMING ORGANIZATION REPORT NUMBER

NRL/MR/4790—92-6973

9. SPONSORING / MONITORING AGENCY NAME(S) AND ADDRESS(ES)

DOE
Washington, DC 20545

10. SPONSORING / MONITORING AGENCY REPORT NUMBER

11. SUPPLEMENTARY NOTES

12a. DISTRIBUTION / AVAILABILITY STATEMENT

Approved for public release; distribution unlimited.

12b. DISTRIBUTION CODE

13. ABSTRACT *(Maximum 200 words)*

A compact laser synchrotron source (LSS) is proposed as a means of generating tunable, narrow bandwidth, ultra-short pulses of hard x-rays. The LSS is based on the Thomson backscattering of intense laser radiation from a counterstreaming electron beam. Advances in both compact ultra-intense solid-state lasers and high brightness rf linac beams make the LSS a very attractive compact source of high brightness x-rays, particularly at photon energies beyond ~ 30 keV. The x-ray wavelength is $\lambda[\text{A}] = 650\ \lambda_o[\mu\text{m}]/E_b^2\ [\text{MeV}]$, where λ_o is the laser wavelength and E_b is the electron beam energy. For $E_b = 72$ MeV and $\lambda_o = 1\ \mu$m, x-rays at $\lambda = 0.12$ Å (100 keV) are generated. The spectral flux, brightness, bandwidth and pulse structure are analyzed. In the absence of filtering the spectral bandwidth in the LSS is typically $\lesssim 1\%$ and is limited by electron beam emittance and energy spread. Two configurations of the LSS are discussed, one providing high peak power and the other high average power. Using present day technology, the LSS can generate single pulses of x-rays consisting of $> 10^9$ photons/pulse with a pulse duration of $\sim$ psec and photon energies from 50-1200 keV. In a highly rep-rated configuration, the LSS can also provide high average brightness ($\sim 10^{13}$ photons/sec-mm^2-mrad^2 (0.1% BW)) hard x-rays (> 50 keV) in a sequence of $\sim$ psec pulses.

14. SUBJECT TERMS

Synchrotron radiation Thomson backscattering
Intense lasers

15. NUMBER OF PAGES

29

16. PRICE CODE

17. SECURITY CLASSIFICATION OF REPORT	18. SECURITY CLASSIFICATION OF THIS PAGE	19. SECURITY CLASSIFICATION OF ABSTRACT	20. LIMITATION OF ABSTRACT
UNCLASSIFIED	UNCLASSIFIED	UNCLASSIFIED	SAR

CONTENTS

TUNABLE, SHORT PULSE HARD X-RAYS FROM A COMPACT LASER SYNCHROTRON SOURCE

I. INTRODUCTION

The development of a compact, tunable, near monochromatic hard x-ray source would have profound and wide ranging applications in a number of areas. These areas include x-ray diagnostics, medical imaging, microscopy, nuclear resonance absorption, solid-state physics and material sciences. The properties of the x-ray beam which are important for these applications include spectral width, spectral brightness, photon flux, pulse configuration and polarization. Presently, third generation synchrotron sources are being pursued which are based on high energy electron storage rings and undulator magnetic fields.[1-10] In the following, a laser synchrotron source (LSS) is proposed in which the magnetic undulator is replaced by ultra-high intensity laser pulses, e.g., from a Nd:YAG/Nd:glass laser, and the electron storage ring is replaced by an electron beam of substantially lower energy, e.g., from an rf linac or a high current betatron. Recent advances in compact, short pulse, high intensity laser technology[11-13] make the LSS a potentially attractive compact source, particularly at high x-ray energies.

In the LSS, the mechanism for generating tunable, near monochromatic, well-collimated hard x-ray radiation is Thomson scattering,[14-17] which is essentially the same as in undulator synchrotron sources. Using present day laser and accelerator technology, it is possible to generate x-ray beams having either high peak or moderate average power. Ultra-short pulses (~ psec duration) of hard x-rays (> 50 keV) consisting of $> 10^9$ photons/pulse can be generated (see Table I). A moderate average power LSS can provide average photon fluxes of $\gtrsim 10^{13}$ photons/sec and an average spectral brightness of $\gtrsim 10^{12}$ photons/sec-mm^2-mrad^2(0.1% BW) (see Table II). The spectral width in the LSS (prior to filtering) is

Manuscript approved May 26, 1992.

limited by the electron beam emittance and energy spread and is typically $\Delta\omega/\bar{\omega}$ ~ 1%. This radiation is well collimated with an angular spread of ~ 1 mrad. The photon energies capable of being generated by the LSS are well beyond the range of present day undulator synchrotron sources. As an example, 100 keV photons (0.12 Å) can be generated using a Nd:YAG laser and a 72 MeV electron beam. Since the LSS radiation has a narrow bandwidth, little unusable radiation, which could damage optics and target samples, is generated. The x-ray pulse structure in the LSS is determined by the electron and laser beam pulse structure and, hence, high intensity x-ray pulses of ~ psec duration can be readily generated. Suitable electron beam accelerators for the LSS include rf linacs and betatrons. High current betatrons are particularly attractive for their high average power capability. Electron beam recovery methods may be employed on rf linac beams to minimize average power requirements. Recirculating rf accelerators, such as a race track microtron, may also be well suited to drive the LSS.

One practical application of the LSS x-ray beam is to significantly enhance the imaging ability of low concentrations of trace elements in the human body. Specifically, it could be used in Digital Differential Angiography (DDA), a new medical x-ray diagnostic concept.[18] This new technique is a differential x-ray absorption diagnostic procedure for imaging blood vessels. In conventional angiography, x-ray imaging of blood vessels is achieved by intravenously injecting an x-ray absorbing substance such as iodine. The available x-ray beams used for imaging are extremely broad band and large doses of both iodine and x-rays are required. In fact, present x-ray beams require an "invasive" injection of iodine directly into the heart. A tunable, near monochromatic x-ray beam, using a

differential x-ray absorption technique, would be a very sensitive diagnostic tool for measuring low concentrations of iodine at a reduced radiation dose. Iodine has a K-edge absorption at a photon energy of ≃ 33 keV. In DDA, two x-ray beams are used: one at 33 keV (energy for peak absorption in iodine) and the other at ~ 30 keV. The mass attenuation coefficients for these two photon energies differ by a factor of ~ 8. The photon flux through the tissue is proportional to the exponent of the mass attenuation coefficient times the mass thickness of the tissue. Therefore, the difference between the 33 keV photon image and the 30 keV photon image is a direct and sensitive measure of the concentration of iodine, while the images of the bones and other tissues not containing the iodine is suppressed. This differential x-ray absorbing technique would use much lower concentrations of iodine injected "non-invasively" into the heart via the bloodstream. The imaging and subtraction of the two x-ray beams would be performed at the same time and, therefore, patient movement during the imaging process would not be a factor.

A relativistic electron beam interacting with an incident counterstreaming laser field emits synchrotron radiation (see Fig. 1). The radiation is predominantly emitted in the direction of the electrons and the frequency is twice doppler shifted upward from the incident laser frequency. The frequency of the LSS radiation along the axis is $\bar{\omega} = 4\gamma_o^2\omega_o$, where ω_o is the incident laser frequency and $\gamma_o >> 1$ is the relativistic factor associated with the electrons. The photon energy, $E_p = h\bar{\omega}/2\pi$, and wavelength are, respectively,

$$E_p[\text{keV}] = 1.9 \times 10^{-2} E_b^2[\text{MeV}]/\lambda_o[\mu\text{m}],$$

$$\lambda[\mathring{A}] = 12.4/E_p[\text{keV}] = 6.5 \times 10^2 \, \lambda_o[\mu\text{m}]/E_b^2[\text{MeV}],$$

where λ is the synchrotron radiation wavelength in units of $\mathring{A}$, E_b is the electron beam energy in units of MeV and λ_o is the incident laser wavelength in units of μm. In the case where the incident laser is a Nd:YAG (or Nd:glass) laser with wavelength $\lambda_o = 1$ μm and the electron beam energy is $E_b = 40$ MeV, radiation is generated with an energy of $E_p = 30$ keV, corresponding to a wavelength of $\lambda = 0.40$ $\mathring{A}$. The tunability of the x-ray energy is achieved by changing the electron beam energy. Notice that by using a $\lambda_o = 1$ μm laser in conjunction with a high energy storage ring ($E_b = 1$ GeV), high brightness gamma-ray ($E_p = 19$ MeV) radiation can be generated.

Conventional synchrotron sources utilizing magnetic undulators (or wigglers) require substantially higher electron beam energies, compared to the LSS, to achieve the same photon energy. Typically, undulator wavelengths are $\gtrsim 10^4$ times longer than laser wavelengths. Therefore, conventional undulator sources require electron beam energies $\gtrsim 100$ times higher than corresponding LSSs. The energy and wavelength of synchrotron radiation from a conventional undulator are, respectively,

$$E_p[\text{keV}] = 0.95 \frac{E_b^2[\text{GeV}]/\lambda_u[\text{cm}]}{(1 + K^2/2)},$$

$$\lambda[\mathring{A}] = 13.0 \frac{\lambda_u[\text{cm}](1 + K^2/2)}{E_b^2[\text{GeV}]},$$

where E_b is the electron beam energy in GeV, λ_u is the undulator wavelength in units of cm and $K \lesssim 1$ is the wiggler strength parameter (deflection parameter). To generate $E_p = 30$ keV photons using a $\lambda_u = 1$ cm undulator period, electron beam energies of $E_b \gtrsim 6$ GeV are needed (~ 150 times higher than needed for a LSS).

An important parameter in the discussion of LSS radiation is the unitless laser strength parameter, a_o, where $a_o = |e|A/m_oc^2$ is the normalized peak amplitude of the laser vector potential, A. The laser strength parameter, analogous to the wiggler strength parameter K, is related to the incident power, P_o, of a linearly polarized laser by

$$P_o[GW] = 21.5(a_o r_o/\lambda_o)^2,$$

where r_o is the spot size of the Gaussian laser profile. The magnitude of the electron transverse quiver velocity is proportional to the laser strength parameter, $v_\perp = ca_o/\gamma_o$, where γ_o is the electron relativistic factor. The peak laser electric field amplitude, E_o, and the laser intensity, $I_o = 2P_o/\pi r_o^2$, are given respectively by $E_o[TeV/m] = 3a_o/\lambda_o[\mu m]$, and $I_o[W/cm^2] = 1.38 \times 10^{18}\ a_o^2/\lambda_o^2[\mu m]$.

Significant advancements have occurred in recent years[11-13] in the development of compact laser systems which deliver modest energy ($\geq$ 1 J), ultra-short ($\leq$ 1 psec) laser pulses at ultra-high powers ($\geq$ 1 TW) and intensities ($\geq 10^{18}$ W/cm^2). These compact laser systems, such as the Table-Top Terawatt (T^3) laser, are based on the technique of chirped-pulse amplification (CPA), first applied to solid-state lasers in 1985.[11] The availability of compact lasers capable of providing picosecond, TW pulses with $a_o \sim 1$, makes the LSS a potentially viable high peak power, hard x-ray source. Although in what follows it is assumed that $a_o < 1$, values of a_o of the order or greater than unity can be achieved. When $a_o < 1$, the LSS radiation from different laser periods interfere coherently resulting in sharp peaks at harmonics of the fundamental frequency $\bar{\omega}$. When $a_o >> 1$, the interference effects are not present, the radiation adds incoherently, and the resulting spectrum is broad.

II. LASER SYNCHROTRON SOURCE

Consider a linearly polarized laser field Thomson scattering off relativistic free electrons. The laser propagates towards the left and interacts with electrons propagating towards the right, i.e., the positive z-direction, as shown in Fig. 1.

The LSS radiation frequency is

$$\omega = \bar{\omega}(1 - \gamma_o^2\theta^2), \tag{1}$$

where $\theta << 1$ is the observation angle with respect to the forward direction and $\bar{\omega} = 4\gamma_o^2\omega_o$ is the frequency along the axis. The spectral width within the cone of half angle θ is

$$\delta\omega/\bar{\omega} \simeq \gamma_o^2\theta^2, \tag{2}$$

and the finite interaction length broadening of the spectral width at a fixed observation angle θ is

$$(\delta\omega/\bar{\omega})_o \simeq 1/N_o, \tag{3}$$

where $N_o = 2L/\lambda_o$ is twice the number of laser wavelengths within the interaction length L. The interaction length, L, which is the distance over which the electrons interact with the laser field, depends on the laser pulse length, L_o, Rayleigh length, $Z_R = \pi r_o^2/\lambda_o$, and/or the laser-electron intersection length, L_{int}. In general, L is given by the minimum of $L_o/2$, $2Z_R$ or L_{int}. One difference between a conventional synchrotron source using an undulator and an LSS is the value of N_o. In the case of the undulator, the number of wiggler periods is typically $< 10^2$ while in the case of the LSS, the number of laser wavelengths can be large, $> 10^3$.

The synchrotron power radiated by a single beam electron interacting with a laser beam is

$$P_s = 21.3\ \gamma_o^2 (r_e/r_o)^2\ P_o, \qquad (4)$$

where $r_e = |e|^2/m_o c^2 = 2.82 \times 10^{-9}$ μm is the classical electron radius. The total peak power radiated by an electron beam interacting with a finite laser pulse is

$$P_T = 21.3\ \frac{fI_b}{|e|}\ \frac{L}{c}\ \frac{r_e^2}{r_o^2}\ \gamma_o^2\ P_o, \qquad (5)$$

where I_b is the electron beam current,

$$f = \begin{cases} A_o/A_b & , \quad A_o < A_b \\ 1 & , \quad A_o > A_b \end{cases}$$

is the filling factor and A_o, A_b are the cross-sectional areas of the laser and electron beam respectively. The total radiated power in practical units is

$$P_T[W] = 4.2 \times 10^{-2} f(L/Z_R)\lambda_o^{-1}[\mu m] I_b[A] E_b^2[MeV] P_o[GW], \qquad (6)$$

where $Z_R = \pi r_o^2/\lambda_o$ is the Rayleigh length of the incident laser. The total efficiency of x-ray power generation with respect to the electron beam power, P_b, is

$$\eta[\%] = P_T/P_b = 4.2 \times 10^{-6} f(L/Z_R)\lambda_o^{-1}[\mu m] E_b[MeV] P_o[GW]. \qquad (7)$$

As an illustration, for the case shown in Table I, where $\lambda_o = 1$ μm, $I_b = 200$ A, $E_b = 50$ MeV, $P_o = 10$ TW (2 psec duration), $L/Z_R = 0.04$ and $f = 1$, the total peak radiated power is $P_T = 8$ MW at a photon energy of

E_p = 48 keV (λ = 0.25 Å) and the efficiency is $\eta = 8 \times 10^{-2}$%. The photon flux is ~ 6×10^{21} photons/sec (6×10^9 photons/pulse for a 1 psec x-ray pulse) and is confined to a cone of angle ~ $1/\gamma \approx 10$ mrad in the forward direction. Note that within this angle the spectral width is large, $\delta\omega/\bar{\omega} \approx 1$.

a) Spectral Intensity

For the case of a single electron emitting synchrotron radiation, the energy radiated per unit solid angle per unit frequency interval is[19]

$$\frac{d^2I}{d\Omega d\omega} = \frac{|e|^2\omega^2}{4\pi^2 c}\left|\int_{-T/2}^{T/2} \underset{\sim}{n}x(\underset{\sim}{n}x\underset{\sim}{\beta})\exp(i\psi)dt\right|^2, \qquad (8)$$

where $\underset{\sim}{n}$ is a unit vector pointing from the radiating electron to the observation point, $\psi = \omega(t - \underset{\sim}{n}\cdot\underset{\sim}{r}/c)$, $\underset{\sim}{r}$ is the electron's coordinate, $\underset{\sim}{\beta} = c^{-1}d\underset{\sim}{r}/dt$, $T = L/c$ is the interaction time and Ω is the solid angle. The intensity distribution in Eq. (8) can be evaluated for relativistic electrons interacting with a counterstreaming laser pulse. The intensity distribution directed in the forward direction, i.e., $\theta = 0$, is found to be

$$\frac{d^2I(o)}{d\Omega d\omega} = \frac{|e|^2\omega^2}{8\pi c^2}\lambda_o N_o a_o^2 S(\omega - \bar{\omega}), \qquad (9)$$

where

$$S(\omega - \bar{\omega}) \begin{cases} \left(N_o/\bar{\omega}\right)\left(\dfrac{\sin\left((\omega - \bar{\omega})\pi N_o/\bar{\omega}\right)}{(\omega - \bar{\omega})\pi N_o/\bar{\omega}}\right)^2 \\ \\ \delta(\omega - \bar{\omega}), \quad \text{for } N_o \to \infty \end{cases}$$

is the spectral width function. The frequency width of the function S is $(\delta\omega/\bar{\omega})_o \approx \lambda_o/2L = 1/N_o$.

The angular density of the spectral flux, i.e., the peak number of photons in the frequency range $\omega_1 \leq \omega \leq \omega_2$ emitted per second per unit solid angle in the forward direction, is given by

$$\frac{dF_o}{d\Omega} = \left(\frac{2\pi}{h\omega}\right) \dot{N}_b \int_{\omega_1}^{\omega_2} d\omega \, \frac{d^2I(o)}{d\Omega d\omega}, \tag{10}$$

where F_o is the spectral flux for an ideal electron beam, i.e., zero emittance and energy spread, $\dot{N}_b = fI_b/|e|$ is the electron flux interacting with the laser beam, I_b is the total beam current, and h is Planck's constant. Evaluating Eq. (10) yields

$$\frac{dF_o}{d\Omega} = (\alpha f I_b/|e|)a_o^2\gamma_o^2 N_o \begin{cases} N_o \Delta\omega/\bar{\omega} & , \text{ for } \Delta\omega/\bar{\omega} \ll 1/N_o \\ 1 & , \text{ for } \Delta\omega/\bar{\omega} \gg 1/N_o, \end{cases} \tag{11}$$

where $\alpha = 2\pi|e|^2/hc = 1/137$ is the fine structure constant and $\Delta\omega/\bar{\omega} = (\omega_2 - \omega_1)/\bar{\omega}$ is the specified spectral width, i.e., the spectral width required for a particular application. In practical units, the peak number of photons emitted per second per square milliradian of solid angle in the forward direction is

$$\frac{dF_o}{d\Omega}\left[\frac{\text{photons}}{\text{sec-mrad}^2}\right] = 5.1 \times 10^{10} f(L/Z_R)\, I_b[A]\, E_b^2[\text{MeV}]\, P_o[\text{GW}]$$

$$\cdot \begin{cases} N_o \Delta\omega/\bar{\omega} & , \text{ for } \Delta\omega/\bar{\omega} \ll 1/N_o \\ 1 & , \text{ for } \Delta\omega/\bar{\omega} \gg 1/N_o, \end{cases} \tag{12}$$

where an ideal electron beam has been assumed. For an ideal electron beam, the spectral flux with spectral width $\Delta\omega/\bar{\omega}$ is $F_o = \int(dF_o/d\Omega)d\Omega$,

$$F_o \simeq 2\pi(\alpha f I_b/|e|)a_o^2 N_o(\Delta\omega/\bar{\omega}), \tag{13}$$

which is valid for all values of $\Delta\omega/\bar{\omega} \lesssim 1$.

b) Electron Beam Emittance and Energy Spread Effects

In actual electron beams, the electrons may have an average angular spread as well as an average energy spread. The beam emittance and intrinsic energy spread associated with the electron beam account for the angular and energy spreads, respectively. The normalized beam emittance is given by $\varepsilon_n = \gamma_o r_b \theta_b$, where r_b is the average electron beam radius and θ_b is the average electron angular spread. The fractional longitudinal beam energy spread due to emittance is

$$(\delta E/E_b)_\varepsilon = \frac{1}{2}\,\varepsilon_n^2/r_b^2. \tag{14}$$

Electron beams may also have an intrinsic energy spread, $(\delta E/E_b)_{int}$, due to various reasons, such as voltage variation, finite pulse length effects, etc.

The total natural spectral width of the LSS radiation is

$$(\delta\omega/\bar{\omega})_T \simeq \left((\delta\omega/\bar{\omega})_o^2 + (\delta\omega/\bar{\omega})_\varepsilon^2 + (\delta\omega/\bar{\omega})_{int}^2\right)^{1/2}, \tag{15}$$

where

$$(\delta\omega/\bar{\omega})_o = 1/N_o \tag{16a}$$

is the finite interaction length spectral width contribution,

$$(\delta\omega/\bar{\omega})_\varepsilon = \varepsilon_n^2/r_b^2 \tag{16b}$$

is the emittance broadened spectral width and

$$(\delta\omega/\bar{\omega})_{int} = 2(\delta E/E_b)_{int} \qquad (16c)$$

is the intrinsic energy spread broadening contribution. The radiation with total spectral width $(\delta\omega/\bar{\omega})_T$ is confined to the angle

$$\theta_T \simeq (\delta\omega/\bar{\omega})_T^{1/2}/\gamma_o. \qquad (17)$$

As an illustration, for an rf linac electron beam with an emittance $\varepsilon_n \simeq 5$ mm-mrad, radius $r_b = 50$ μm and $\gamma_o = 100$, the longitudinal energy spread due to emittance is $(\delta E/E_b)_\varepsilon \simeq 0.5\%$, and the emittance broadened spectral width is $(\delta\omega/\bar{\omega})_\varepsilon \simeq 1\%$. Since the intrinsic energy spread is typically ~ 1% and $N_o \gtrsim 10^4$, the total spectral width of the unfiltered LSS radiation is typically $(\delta\omega/\bar{\omega})_T \simeq 1\%$ and is confined to the angle $\theta_T \simeq 1$ mrad. If a bandwidth $\Delta\omega/\bar{\omega} >> (\delta\omega/\bar{\omega})_T$ is required, all the radiation within a cone of half-angle $\theta_s = (\Delta\omega/\bar{\omega})^{1/2}/\gamma_o$ can be used. To obtain a bandwidth $\Delta\omega/\bar{\omega} << (\delta\omega/\bar{\omega})_T$, the radiation within the cone θ_T must be filtered using a monochromator.

To account for the effects of electron angular and energy spread, Eq. (8) must be solved using non-ideal electron trajectories and distributions. The dominant dependence on angles, emittance and energy spread enters through the spectral width function S. The effects of emittance, energy spread and angular variation in Eq. (9) is approximately accounted for by replacing $\bar{\omega}$ in the spectral width function, S, with $\bar{\omega}(1 - \gamma^2(\theta-\theta_b)^2 - 2(\delta E/E_b)_{int})$.

c) Spectral Flux and Brightness

A fundamental quantity which is important in characterizing radiation is the spectral brightness. The spectral brightness is the phase space

density of the spectral flux, i.e., the number of photons emitted per second per unit source area, per unit solid angle, within a given bandwidth. The electron angular spread and energy spread can play an important role in affecting the spectral flux and brightness of the LSS radiation. The spectral flux of the LSS radiation beam is the total number of photons per second emitted with a given spectral width $\Delta\omega/\bar{\omega}$ about the frequency $\bar{\omega}$ and is given by

$$F = \int \frac{dF}{d\Omega}\, d\Omega, \simeq (dF/d\Omega)2\pi\theta_R^2, \tag{18}$$

where $\Omega \simeq 2\pi\theta_R^2$ is the solid angle and $\theta_R \simeq (\theta_s^2 + \theta_T^2)^{1/2} = (\Delta\omega/\bar{\omega} + (\delta\omega/\bar{\omega})_T)^{1/2}/\gamma_o$ is the cone angle containing the radiation of specified spectral width. The spectral brightness is the phase space density of F and is given by

$$B = \frac{F}{(2\pi)^2(\sigma_R\theta_R)^2} \simeq (dF/d\Omega)/(2\pi\sigma_R^2), \tag{19}$$

where $(\sigma_R\theta_R)^2$ is the phase space area of the photon beam, i.e., σ_R is the total effective size of the radiation source. The quantity σ_R is given by

$$\sigma_R \simeq (r_s^2 + (\theta_R L/2)^2)^{1/2}, \tag{20}$$

where $r_s = \min(r_b, r_o)$ is the minimum spot size of the radiation, $L = \lambda_o N_o/2$ and the spectral width of the radiation determines the radiation angle, θ_R.

The spectral flux within the spectral width $\Delta\omega/\bar{\omega}$ is the same for a non-ideal electron beam as it is for an ideal beam, i.e., $F = F_o$ within $\Delta\omega/\bar{\omega} \lesssim 1$. The spectral flux and brightness for a non-ideal electron beam are

$$F = 2\pi(\alpha f I_b/|e|)a_o^2 N_o(\Delta\omega/\bar{\omega}), \tag{21a}$$

$$B = \frac{\alpha f}{2\pi r_s^2}\frac{I_b}{|e|}\frac{a_o^2\gamma_o^2 N_o}{(1+\delta)}\frac{\Delta\omega/\bar{\omega}}{\left(\Delta\omega/\bar{\omega} + (\delta\omega/\bar{\omega})_T\right)}. \tag{21b}$$

where $\delta = (\theta_R L/2r_s)^2$. In practical units

$$F\left[\frac{\text{photons}}{\text{sec}}\right] = 8.4 \times 10^{16} f(L/Z_R) I_b[A] P_o[GW](\Delta\omega/\bar{\omega}), \tag{22a}$$

$$B\left[\frac{\text{photons}}{\text{sec-mm}^2\text{-mrad}^2}\right] = 8.1 \times 10^9 f(L/Z_R)$$

$$\cdot \frac{I_b[A]\ E_b^2[\text{MeV}]\ P_o[GW]}{r_s^2[\text{mm}]}\frac{(\Delta\omega/\bar{\omega})/(1+\delta)}{\Delta\omega/\bar{\omega} + (\delta\omega/\bar{\omega})_T}, \tag{22b}$$

where $\delta = (L/2\gamma_o r_s)^2(\Delta\omega/\bar{\omega} + (\delta\omega/\bar{\omega})_T)$ is typically $<< 1$. The average spectral flux and brightness are given by $\langle F\rangle = DF$ and $\langle B\rangle = DB$, respectively, where D is the duty factor associated with the particular LSS configuration. The x-ray pulse structure depends on L_o, Z_R, L_{int} and/or the electron beam pulse length, L_b. Specific examples will be given in the following section.

III. LSS CONFIGURATION

Two configurations will be discussed: a) a high peak power LSS utilizing an rf linac and b) a moderate average power LSS utilizing an rf linac or a betatron accelerator.

a) High Peak Power LSS

In a high peak power LSS, picosecond x-ray pulses are generated by the picosecond electron micropulses from an rf linac. It has been implicitly assumed that all the electrons in the micropulse are acted on by approximately the same incident laser field amplitude. This requires that the electron beam micropulse length be somewhat less than the laser Rayleigh length, i.e., $L_b < Z_R$. To maintain a somewhat uniform intensity along the laser pulse, the laser pulse length should be approximately equal to the Rayleigh length, i.e., $L_o \simeq Z_R$. In addition, for high efficiency operation the spot size of the incident laser beam should be somewhat larger than the electron beam radius, i.e., $r_o \gtrsim r_b$.

The slippage between the x-ray pulse and the electron micropulse is negligibly small compared to the electron micropulse length. Hence, the x-ray pulse structure is essentially identical to that of the electron beam pulse structure, i.e., psec electron pulses generate psec x-ray pulses. Both the electron and x-ray pulse are overlapped and travel together at nearly the velocity of light through the counterstreaming incident laser pulse. Ultra-short x-ray pulses (~ psec) can also be generated using long electron pulses (>> psec). This is accomplished by appropriately adjusting the incident laser's Rayleigh length, pulse length and/or angle of incidence.

For single-pulse, high peak power x-rays, the laser system most suitable for the LSS is the T^3 laser system. In the T^3 laser, a low energy pulse from an ultra-short pulse, mode-locked oscillator is temporally stretched, amplified, and recompressed by the CPA technique to produce a ~ 1 psec laser pulse with peak laser power in the 1-10 TW range. Presently, T^3 lasers can be rep-rated[13] up to ~ 1 kHz at the ~ 1 TW level.

Synchronization between the single laser pulse and the rf linac electron beam can be achieved with a laser-triggered photocathode at the beam injector of the accelerator. Part of the laser pulse from the T^3 laser can be diverted to illuminate the photocathode of the rf linac. Table I shows the parameters for a high peak power LSS using a rf linac in which psec x-ray pulses with 6×10^9 photons/pulse are generated.

b) Moderate Average Power LSS

A moderate average power LSS can be realized by using either a rep-rated rf linac or a CW betatron. A rep-rated rf linac consists of a series of micropulses and macropulses. In typical rf linacs, the micropulse time is $\tau_m = L_b/c \simeq 10$ psec and the macropulse time is $T_m \simeq 20$ μsec. The micropulse and macropulse rep rate is typically $f_m \simeq 3$ GHz and $F_m \simeq 100$ Hz, respectively. The separation of the micropulse is $\Delta T_m = 1/f_m \simeq 350$ psec and the overall duty factor for the full electron pulse train is $D = F_m f_m T_m \tau_m \simeq 6 \times 10^{-5}$.

Due to the relatively low duty factor ($D \simeq 10^{-5}$) associated with rf linacs, a rep-rated LSS requires a laser system that has high average power. An attractive approach is to employ a pulsed laser configuration rep-rated at the frequency of the electron micropulses. As shown in Fig. 2, the laser pulse train is arranged to circulate in a ring resonator

configuration with an optical path length which is an integral multiple of ΔT_m. A low gain amplifier supplies the mirror and diffraction losses. The electron beam micropulses are brought into one arm of the laser resonator with a turning magnet and synchronized with the laser pulses so that they interact with each other in the vicinity of the focal point. Synchronization between the laser pulses and electron pulses is achieved by driving the laser mode-locked oscillator at subharmonics of the master oscillator signal of the rf linac.

Betatron accelerators can provide both high current and high energy compact electron beams for the LSS. Conventional air core betatrons have produced ~ 100 A of circulating current at energies of ~ 50 MeV.[20] These betatrons were extremely compact, varying in radius from ~ 4-24 cm. To stably confine and accelerate high currents, the modified betatron was proposed.[21] The modified betatron, which has additional stabilizing magnetic fields,[21,22] has recently accelerated > 1 kA to energies of > 20 MeV.[23] The beam radius in the modified betatron is 1 m.

For a moderate average power LSS using a conventional betatron, it is not necessary to employ a short-pulsed rep-rated laser system because the electron beam is continuous. A ring resonator can be completely filled with a laser pulse of the same length as the resonator. A schematic of the LSS betatron configuration is shown in Fig. 3. Assuming a 2% loss of laser power due to mirrors and diffractions, the CW laser power in the ring resonator can be as high as 5 kW for an input laser amplifier power of ~ 100 W. The interaction distance L is given by $L = L_{int} \simeq (2Rr_b)^{1/2}$ where R is the major radius of the betatron and r_b is the horizontal radius of the electron beam. An average spectral brightness of ~ 3×10^{11} photons/sec-$mm^2 mrad^2$(0.1% BW) at x-ray photon energy of 50 keV can be obtained. Due to

the CW nature of both the electron and laser beams, the duty factor is equal to 1. This leads to an increase of the average photon flux, when compared to the moderate average power LSS using an rf linac. Table II shows the parameters for a moderate average power LSS using a conventional betatron.

IV. CONCLUSION

Advances in ultra-high power lasers make possible the generation of hard x-rays using relatively low energy electron beams. The LSS has a number of potentially unique and attractive features which may serve a variety of applications. These features include compactness, relatively low cost, tunability, narrow bandwidth, short pulse structure, high photon energy operation and high levels of photon flux and brightness. The relatively narrow natural linewidth associated with the LSS can provide less unusable radiation which could damage optics and target samples. In addition, by varying the electron pulse energy, chirped x-ray pulses may be generated. The pulse structure, tunability and high photon energy capability of the LSS may provide an important tool for studying ultra-fast phenomena. Furthermore, the relatively low cost and compactness of a LSS can make synchrotron light sources more readily available to users.

Acknowledgments

This work has been supported by the Office of Naval Research, the Medical FEL Program, and the Department of Energy. The authors would like to thank G. Mourou for useful discussions and suggestions concerning high power laser systems.

REFERENCES

1. K. J. Kim, in "Physics of Particle Accelerators", edited by M. Month and M. Dienes, AIP Conf. Proc. 184 (Amer. Inst. Physics, New York, 1989), Vol. I, p. 565.
2. H. Winick, ibid., Vol II, P. 2138.
3. S. Krinsky, in Proc. 1991 IEEE Particle Accelerator Conf., edited by M. Allen (IEEE, New York, 1991), Vol. I, p. 11.
4. A. Jackson, ibid., Vol. IV, p. 2637; A. L. Robinson and A. S. Schlachter, ibid., Vol IV, p. 2640.
5. B. G. Levi, Physics Today 44, 17 (1991).
6. H. Winick, Scientific American 225, 88 (1987).
7. B. M. Kincaid, J. Appl. Phys. 48, 2684 (1977).
8. S. K. Ride and W. B. Colson, Stanford University High Energy Physics Lab Report 858 (1979).
9. R. Coisson, IEEE J. Quantum Electron. QE-17, 1409 (1981).
10. W. B. Colson, G. Dattoli and F. Ciocci, Phys. Rev. A 31, 828 (1985).
11. D. Strickland and G. Mourou, Opt. Commun. 56, 216 (1985); P. Maine, D. Strickland, P. Bado, M. Pessot and G. Mourou, IEEE J. Quantum Electron. QE-24, 398 (1988); J. Squier, F. Salin, G. Mourou and D. Harter, Opt. Lett. 16, 324 (1991).
12. M. D. Perry, F. G. Patterson and J. Weston, Opt. Lett. 15, 1400 (1990); F. G. Patterson and M. Perry, J. Opt. Soc. Am. B 8, 2384 (1991).
13. F. Salin, J. Squier and G. Vaillancourt, Opt. Lett. 16, 1964 (1992); D. Umstadter, private communication.
14. E. S. Sarachik and G. T. Schappert, Phys. Rev. D 1, 2738 (1970).
15. P. Sprangle, B. Hafizi and F. Mako, Appl. Phys. Lett. 55, 2559 (1989).

16. F. Carroll, J. Waters, R. Price, C. Brau, C. Roos, N. Tolk, D. Pickens and H. Stephens, Investigative Radiology 25, 465 (1990).

17. P. Sprangle and E. Esarey, NRL Memorandum Report 6949, accepted by Phys. Fluids (1992).

18. P. R. Moran, R. J. Nickles and J. A. Zagzebski, Physics Today, July (1983).

19. J. D. Jackson, "Classical Electrodynamics", (Wiley, New York, 1975), Chap. 14.

20. A. I. Pavlovskii, et al., Sov. Phys. Tech. Phys. 22, 218 (1977).

21. P. Sprangle and C. A. Kapetanakos, J. Appl. Phys. 49, 1 (1978).

22. C. W. Roberson, A. Mondelli and D. Chernin, Phys. Rev. Lett. 50, 507 (1983).

23. C. A. Kapetanakos, et al., Phys. Rev. Lett. 64, 2374 (1990) and private communications with C. A. K.

Table I

High Peak Power Laser Synchrotron Source Using an RF Linac

Incident Laser Parameters

Wavelength, λ_o	1 μm
Energy/Pulse, E_o	20 J
Peak Power, P_o	10 TW
Laser Pulse Length, L_o/c	2 psec
Spot size, r_o	50 μm
Rayleigh Length, Z_R	0.8 cm

Electron Pulse Parameters

Beam Energy, E_b	50-250 MeV
Beam Current, I_b	200 A
Beam Pulse Length, L_b/c	1 psec
Beam Radius, r_b	50 μm
Beam Energy Spread $(\Delta E/E_b)_{int}$	0.5%
Beam Emittance, ε_n	5 mm-mrad

X-Ray Pulse Parameters

Photon Energy, E_p	50-1200 keV
Peak Photon Flux, F	6×10^{21} photons/sec (*)
Photon Pulse Length, L_b/c	1 psec
Photons/Pulse, FL_b/c	6×10^{9} photons/pulse (*)
Peak Brightness, B	6×10^{19} - 1.5×10^{21} (+)
Angular Spread, $\theta \sim 1/\gamma$	10-2 mrad

(*) Includes all photons within the $\sim 1/\gamma$ angle, implying ~ 100% BW.

(+) The unit for brightness is photons/sec-mm^2-mrad^2(0.1% BW).

Table II

Moderate Average Power Laser Synchrotron Source Using a Conventional Betatron

Incident Laser Parameters

Wavelength, λ_o	1 μm
Average Circulating Power, P_o	5 kW
Average Laser Amplifier Power, P_{in}	100 W
Spot size, r_o	50 μm
Rayleigh Length, Z_R	0.8 cm

Electron Pulse Parameters

Beam Energy, E_b	50-250 MeV
Beam Current, I_b	100 A
Beam Major Radius, R	25 cm
Beam Cross-section, A_b	πx50x150 μm^2
Interaction Distance, L	1.7 cm
Beam Energy Spread $(\Delta E/E_b)_{int}$	1%

X-Ray Pulse Parameters

Photon Energy, E_p	50-1200 keV
Average Photon Flux, <F>	$3x10^{13}$ photons/sec (*)
Average Spectral Brightness, <B>	$3x10^{11}$ - $7.5x10^{12}$ (+)

(*) Includes all photons within the ~ $1/\gamma$ angle, implying ~ 100% BW.

(+) The unit for brightness is photons/sec-mm^2-$mrad^2$(0.1% BW).

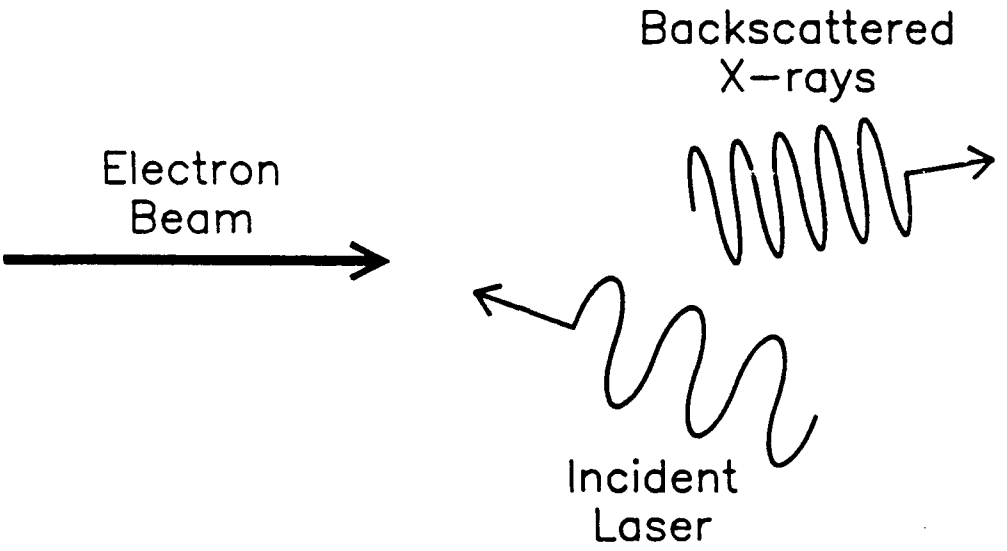

Fig. 1 — Schematic diagram showing the Thomson scattering of an incident beam off a relativistic electron beam to generate x-rays

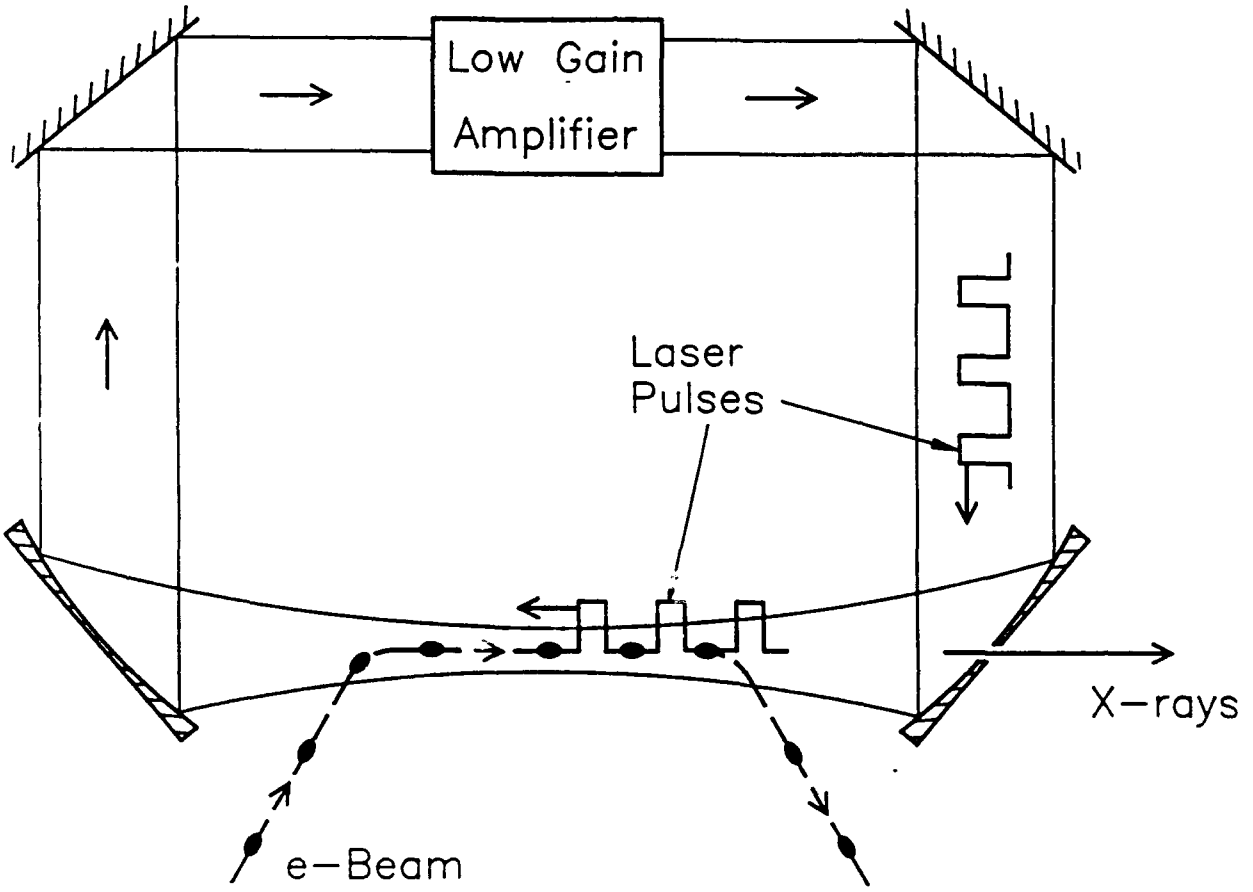

Fig. 2 — Schematic diagram showing a moderate average power LSS driven by an rf linac. The electron pulse train is synchronized with the laser pulse train within the ring resonator.

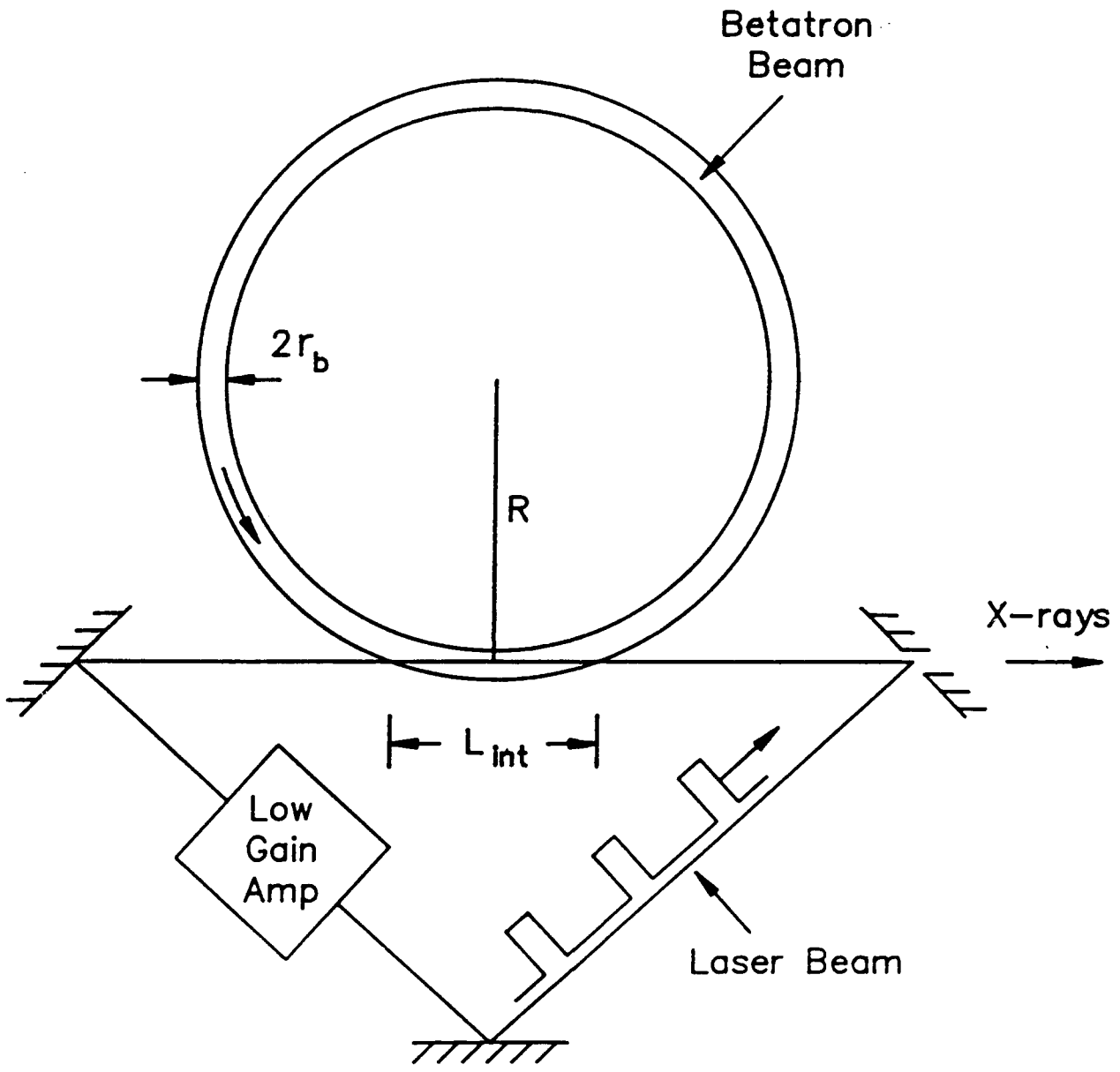

Fig. 3 — Schematic diagram showing a moderate power LSS driven by a betatron.